

Measurement of $\mathcal{B}(t \rightarrow Wb)/\mathcal{B}(t \rightarrow Wq)$ at $\sqrt{s} = 1.96$ TeV

DØ Collaboration

V.M. Abazov^{ak}, B. Abbott^{by}, M. Abolins^{bo}, B.S. Acharya^{ad}, M. Adams^{bb}, T. Adams^{az}, M. Agelou^s, J.-L. Agram^t, S.H. Ahn^{af}, M. Ahsan^{bi}, G.D. Alexeev^{ak}, G. Alkhazov^{ao}, A. Alton^{bn}, G. Alverson^{bm}, G.A. Alves^b, M. Anastasoiaie^{aj}, T. Andeen^{bd}, S. Anderson^{av}, B. Andrieu^r, M.S. Anzelc^{bd}, Y. Arnoud^o, M. Arov^{bc}, A. Askew^{az}, B. Åsman^{ap,aq}, A.C.S. Assis Jesus^c, O. Atramentov^{bg}, C. Autermann^v, C. Avilaⁱ, C. Ay^y, F. Badaudⁿ, A. Baden^{bk}, L. Bagby^{bc}, B. Baldin^{ba}, D.V. Bandurin^{ak}, P. Banerjee^{ad}, S. Banerjee^{ad}, E. Barberis^{bm}, P. Bargassa^{cd}, P. Baringer^{bh}, C. Barnes^{at}, J. Barreto^b, J.F. Bartlett^{ba}, U. Bassler^r, D. Bauer^{be}, A. Bean^{bh}, M. Begalli^c, M. Begel^{bu}, A. Bellavance^{bq}, J. Benitez^{bo}, S.B. Beri^{ab}, G. Bernardi^r, R. Bernhard^{ar}, L. Berntzon^p, I. Bertram^{as}, M. Besançon^s, R. Beuselinck^{at}, V.A. Bezzubov^{an}, P.C. Bhat^{ba}, V. Bhatnagar^{ab}, M. Binder^z, C. Biscarat^{as}, K.M. Black^{bl}, I. Blackler^{at}, G. Blazey^{bc}, F. Blekman^{at}, S. Blessing^{az}, D. Bloch^t, U. Blumenschein^x, A. Boehnlein^{ba}, O. Boeriu^{bf}, T.A. Bolton^{bi}, F. Borchering^{ba}, G. Borissov^{as}, K. Bos^{ai}, T. Bose^{bt}, A. Brandt^{cb}, R. Brock^{bo}, G. Brooijmans^{bt}, A. Bross^{ba}, D. Brown^{cb}, N.J. Buchanan^{az}, D. Buchholz^{bd}, M. Buehler^{ce}, V. Buescher^x, S. Burdin^{ba}, S. Burke^{av}, T.H. Burnett^{cf}, E. Busato^r, C.P. Buszello^{at}, J.M. Butler^{bl}, S. Calvet^p, J. Cammin^{bu}, S. Caron^{ai}, W. Carvalho^c, B.C.K. Casey^{ca}, N.M. Cason^{bf}, H. Castilla-Valdez^{ah}, S. Chakrabarti^{ad}, D. Chakraborty^{bc}, K.M. Chan^{bu}, A. Chandra^{ad}, D. Chapin^{ca}, F. Charles^t, E. Cheu^{av}, F. Chevallier^o, D.K. Cho^{bl}, S. Choi^{ag}, B. Choudhary^{ac}, L. Christofek^{bh}, D. Claes^{bq}, B. Clément^t, C. Clément^{ap,aq,*}, Y. Coadou^{e,f}, M. Cooke^{cd}, W.E. Cooper^{ba}, D. Coppage^{bh}, M. Corcoran^{cd}, M.-C. Cousinou^p, B. Cox^{au}, S. Crépe-Renaudin^o, D. Cutts^{ca}, M. Cwiok^{ae}, H. da Motta^b, A. Das^{bl}, M. Das^{bj}, B. Davies^{as}, G. Davies^{at}, G.A. Davis^{bd}, K. De^{cb}, P. de Jong^{ai}, S.J. de Jong^{aj}, E. De La Cruz-Burelo^{bn}, C. De Oliveira Martins^c, J.D. Degenhardt^{bn}, F. Déliot^s, M. Demarteau^{ba}, R. Demina^{bu}, P. Demine^s, D. Denisov^{ba}, S.P. Denisov^{an}, S. Desai^{bv}, H.T. Diehl^{ba}, M. Diesburg^{ba}, M. Doidge^{as}, H. Dong^{bv}, S. Doulas^{bm}, L.V. Dudko^{am}, L. Dufлот^q, S.R. Dugad^{ad}, A. Duperrin^p, J. Dyer^{bo}, A. Dyshkant^{bc}, M. Eads^{bq}, D. Edmunds^{bo}, T. Edwards^{au}, J. Ellison^{ay}, J. Elmsheuser^z, V.D. Elvira^{ba}, S. Eno^{bk}, P. Ermolov^{am}, J. Estrada^{ba}, H. Evans^{be}, A. Evdokimov^{al}, V.N. Evdokimov^{an}, S.N. Fatakia^{bl}, L. Feligioni^{bl}, A.V. Ferapontov^{an}, T. Ferbel^{bu}, F. Fiedler^z, F. Filthaut^{aj}, W. Fisher^{ba}, H.E. Fisk^{ba}, I. Fleck^x, M. Ford^{au}, M. Fortner^{bc}, H. Fox^x, S. Fu^{ba}, S. Fuess^{ba}, T. Gadfort^{cf}, C.F. Galea^{aj}, E. Gallas^{ba}, E. Galyaev^{bf}, C. Garcia^{bu}, A. Garcia-Bellido^{cf}, J. Gardner^{bh}, V. Gavrilov^{al}, A. Gay^t, P. Gayⁿ, D. Gelé^t, R. Gelhaus^{ay}, C.E. Gerber^{bb}, Y. Gershtein^{az}, D. Gillberg^{e,f}, G. Ginther^{bu}, T. Golling^w, N. Gollub^{ap,aq}, B. Gómezⁱ, K. Gounder^{ba}, A. Goussiou^{bf}, P.D. Grannis^{bv}, S. Greder^c, H. Greenlee^{ba}, Z.D. Greenwood^{bj}, E.M. Gregores^d, G. Grenier^u, Ph. Grisⁿ, J.-F. Grivaz^q, S. Grünendahl^{ba}, M.W. Grünewald^{ae}, J. Guo^{bv}, G. Gutierrez^{ba}, P. Gutierrez^{by}, A. Haas^{bt}, N.J. Hadley^{bk}, P. Haefner^z, S. Hagopian^{az}, J. Haley^{br}, I. Hall^{by}, R.E. Hall^{ax}, L. Han^h, K. Hanagaki^{ba}, K. Harder^{bi}, A. Harel^{bu}, R. Harrington^{bm},

J.M. Hauptman^{bg}, R. Hauser^{bo}, J. Hays^{bd}, T. Hebbeker^v, D. Hedin^{bc}, J.G. Hegeman^{ai},
 J.M. Heinmiller^{bb}, A.P. Heinson^{ay}, U. Heintz^{bl}, C. Hensel^{bh}, G. Hesketh^{bm}, M.D. Hildreth^{bf},
 R. Hirosky^{ce}, J.D. Hobbs^{bv}, B. Hoeneisen^m, M. Hohlfeld^q, S.J. Hong^{af}, R. Hooper^{ca}, P. Houben^{ai},
 Y. Hu^{bv}, V. Hynek^j, I. Iashvili^{bs}, R. Illingworth^{ba}, A.S. Ito^{ba}, S. Jabeen^{bh}, M. Jaffré^q, S. Jain^{by},
 K. Jakobs^x, C. Jarvis^{bk}, A. Jenkins^{at}, R. Jesik^{at}, K. Johns^{av}, C. Johnson^{bt}, M. Johnson^{ba},
 A. Jonckheere^{ba}, P. Jonsson^{at}, A. Juste^{ba}, D. Käfer^v, S. Kahn^{bw}, E. Kajfasz^p, A.M. Kalinin^{ak},
 J.M. Kalk^{bj}, J.R. Kalk^{bo}, D. Karmanov^{am}, J. Kasper^{bl}, I. Katsanos^{bt}, D. Kau^{az}, R. Kaur^{ab},
 R. Kehoe^{cc}, S. Kermiche^p, S. Kesisoglou^{ca}, A. Khanov^{bz}, A. Kharchilava^{bs}, Y.M. Kharzhev^{ak},
 D. Khatidze^{bt}, H. Kim^{cb}, T.J. Kim^{af}, M.H. Kirby^{aj}, B. Klima^{ba}, J.M. Kohli^{ab}, J.-P. Konrath^x,
 M. Kopal^{by}, V.M. Korablev^{an}, J. Kotcher^{bw}, B. Kothari^{bt}, A. Koubarovsky^{am}, A.V. Kozelov^{an},
 J. Kozminski^{bo}, A. Kryemadhi^{ce}, S. Krzywdzinski^{ba}, T. Kuhl^y, A. Kumar^{bs}, S. Kunori^{bk},
 A. Kupco^l, T. Kurča^{u,1}, J. Kvita^j, S. Lager^{ap,aq}, S. Lammers^{bt}, G. Landsberg^{ca}, J. Lazoflores^{az},
 A.-C. Le Bihan^t, P. Lebrun^u, W.M. Lee^{bc}, A. Leflat^{am}, F. Lehner^{ar}, C. Leonidopoulos^{bt}, V. Lesneⁿ,
 J. Leveque^{av}, P. Lewis^{at}, J. Li^{cb}, Q.Z. Li^{ba}, J.G.R. Lima^{bc}, D. Lincoln^{ba}, J. Linnemann^{bo},
 V.V. Lipaev^{an}, R. Lipton^{ba}, L. Lobo^{at}, A. Lobodenko^{ao}, M. Lokajicek^l, A. Lounis^t, P. Love^{as},
 H.J. Lubatti^{cf}, M. Lynker^{bf}, A.L. Lyon^{ba}, A.K.A. Maciel^b, R.J. Madaras^{aw}, P. Mättig^{aa}, C. Magass^v,
 A. Magerkurth^{bn}, A.-M. Magnan^o, N. Makovec^q, P.K. Mal^{bf}, H.B. Malbouisson^c, S. Malik^{bq},
 V.L. Malyshev^{ak}, H.S. Mao^g, Y. Maravin^{bi}, M. Martens^{ba}, S.E.K. Mattingly^{ca}, R. McCarthy^{bv},
 R. McCroskey^{av}, D. Meder^y, A. Melnitchouk^{bp}, A. Mendes^p, L. Mendozaⁱ, M. Merkin^{am},
 K.W. Merritt^{ba}, A. Meyer^v, J. Meyer^w, M. Michaut^s, H. Miettinen^{cd}, J. Mitrevski^{bt}, J. Molina^c,
 N.K. Mondal^{ad}, J. Monk^{au}, R.W. Moore^{e,f}, T. Moulik^{bh}, G.S. Muanza^q, M. Mulders^{ba}, L. Mundim^c,
 Y.D. Mutaf^{bv}, E. Nagy^p, M. Naimuddin^{ac}, M. Narain^{bl}, N.A. Naumann^{aj}, H.A. Neal^{bn}, J.P. Negretⁱ,
 S. Nelson^{az}, P. Neustroev^{ao}, C. Noeding^x, A. Nomerotski^{ba}, S.F. Novaes^d, T. Nunnemann^z,
 E. Nurse^{au}, V. O'Dell^{ba}, D.C. O'Neil^{e,f}, G. Obrant^{ao}, V. Oguri^c, N. Oliveira^c, N. Oshima^{ba},
 R. Otec^k, G.J. Otero y Garzón^{bb}, M. Owen^{au}, P. Padley^{cd}, N. Parashar^{ba,2}, S.K. Park^{af}, J. Parsons^{bt},
 R. Partridge^{ca}, N. Parua^{bv}, A. Patwa^{bw}, G. Pawloski^{cd}, P.M. Perea^{ay}, E. Perez^s, P. Pétrouff^q,
 M. Petteni^{at}, R. Piegaia^a, M.-A. Pleier^w, P.L.M. Podesta-Lerma^{ah}, V.M. Podstavkov^{ba},
 Y. Pogorelov^{bf}, M.-E. Pol^b, A. Pompoš^{by}, B.G. Pope^{bo}, A.V. Popov^{an}, W.L. Prado da Silva^c,
 H.B. Prosper^{az}, S. Protopopescu^{bw}, J. Qian^{bn}, A. Quadt^w, B. Quinn^{bp}, K.J. Rani^{ad}, K. Ranjan^{ac},
 P.A. Rapidis^{ba}, P.N. Ratoff^{as}, P. Renkel^{cc}, S. Reucroft^{bm}, M. Rijssenbeek^{bv}, I. Ripp-Baudot^t,
 F. Rizatdinova^{bz}, S. Robinson^{at}, R.F. Rodrigues^c, C. Royon^s, P. Rubinov^{ba}, R. Ruchti^{bf}, V.I. Rud^{am},
 G. Sajot^o, A. Sánchez-Hernández^{ah}, M.P. Sanders^{bk}, A. Santoro^c, G. Savage^{ba}, L. Sawyer^{bj},
 T. Scanlon^{at}, D. Schaile^z, R.D. Schamberger^{bv}, Y. Scheglov^{ao}, H. Schellman^{bd}, P. Schieferdecker^z,
 C. Schmitt^{aa}, C. Schwanenberger^w, A. Schwartzman^{br}, R. Schwienhorst^{bo}, S. Sengupta^{az},
 H. Severini^{by}, E. Shabalina^{bb}, M. Shamim^{bi}, V. Shary^s, A.A. Shchukin^{an}, W.D. Shephard^{bf},
 R.K. Shivpuri^{ac}, D. Shpakov^{bm}, V. Siccaldi^t, R.A. Sidwell^{bi}, V. Simak^k, V. Sirotenko^{ba},
 P. Skubic^{by}, P. Slattery^{bu}, R.P. Smith^{ba}, G.R. Snow^{bq}, J. Snow^{bx}, S. Snyder^{bw},
 S. Söldner-Rembold^{au}, X. Song^{bc}, L. Sonnenschein^r, A. Sopczak^{as}, M. Sosebee^{cb}, K. Soustruznik^j,
 M. Souza^b, B. Spurlock^{cb}, J. Stark^o, J. Steele^{bj}, K. Stevenson^{be}, V. Stolin^{al}, A. Stone^{bb},
 D.A. Stoyanova^{an}, J. Strandberg^{ap,aq}, M.A. Strang^{bs}, M. Strauss^{by}, R. Ströhmer^z, D. Strom^{bd},
 M. Strovink^{aw}, L. Stutte^{ba}, S. Sumowidagdo^{az}, A. Sznajder^c, M. Talby^p, P. Tamburello^{av},
 W. Taylor^{e,f}, P. Telford^{au}, J. Temple^{av}, B. Tiller^z, M. Titov^x, V.V. Tokmenin^{ak}, M. Tomoto^{ba},
 T. Toole^{bk}, I. Torchiani^x, S. Towers^{as}, T. Trefzger^y, S. Trincaz-Duvold^f, D. Tsybychev^{bv},
 B. Tuchming^s, C. Tully^{br}, A.S. Turcot^{au}, P.M. Tuts^{bt}, R. Unalan^{bo}, L. Uvarov^{ao}, S. Uvarov^{ao},
 S. Uzunyan^{bc}, B. Vachon^{e,f}, P.J. van den Berg^{ai}, R. Van Kooten^{be}, W.M. van Leeuwen^{ai},

N. Varelas^{bb}, E.W. Varnes^{av}, A. Vartapetian^{cb}, I.A. Vasilyev^{an}, M. Vaupel^{aa}, P. Verdier^u,
 L.S. Vertogradov^{ak}, M. Verzocchi^{ba}, F. Villeneuve-Segulier^{at}, J.-R. Vlimant^r, E. Von Toerne^{bi},
 M. Voutilainen^{bq,3}, M. Vreeswijk^{ai}, H.D. Wahl^{az}, L. Wang^{bk}, J. Warchol^{bf}, G. Watts^{cf}, M. Wayne^{bf},
 M. Weber^{ba}, H. Weerts^{bo}, N. Vermes^w, M. Wetstein^{bk}, A. White^{cb}, V. White^{ba}, D. Wicke^{aa},
 D.A. Wijngaarden^{aj}, G.W. Wilson^{bh}, S.J. Wimpenny^{ay}, M. Wobisch^{ba}, J. Womersley^{ba},
 D.R. Wood^{bm}, T.R. Wyatt^{au}, Y. Xie^{ca}, N. Xuan^{bf}, S. Yacoob^{bd}, R. Yamada^{ba}, M. Yan^{bk},
 T. Yasuda^{ba}, Y.A. Yatsunenko^{ak}, Y. Yen^{aa}, K. Yip^{bw}, H.D. Yoo^{ca}, S.W. Youn^{bd}, J. Yu^{cb},
 A. Yurkewicz^{bv}, A. Zatserklyaniy^{bc}, C. Zeitnitz^{aa}, D. Zhang^{ba}, T. Zhao^{cf}, Z. Zhao^{bn}, B. Zhou^{bn},
 J. Zhu^{bv}, M. Zielinski^{bu}, D. Zieminska^{be}, A. Zieminski^{be}, V. Zutshi^{bc}, E.G. Zverev^{am}

^a Universidad de Buenos Aires, Buenos Aires, Argentina

^b LAFEX, Centro Brasileiro de Pesquisas Físicas, Rio de Janeiro, Brazil

^c Universidade do Estado do Rio de Janeiro, Rio de Janeiro, Brazil

^d Instituto de Física Teórica, Universidade Estadual Paulista, São Paulo, Brazil

^e University of Alberta, Edmonton, Alberta, Canada, Simon Fraser University, Burnaby, BC, Canada

^f York University, Toronto, Ontario, Canada, and McGill University, Montreal, PQ, Canada

^g Institute of High Energy Physics, Beijing, People's Republic of China

^h University of Science and Technology of China, Hefei, People's Republic of China

ⁱ Universidad de los Andes, Bogotá, Colombia

^j Center for Particle Physics, Charles University, Prague, Czech Republic

^k Czech Technical University, Prague, Czech Republic

^l Center for Particle Physics, Institute of Physics, Academy of Sciences of the Czech Republic, Prague, Czech Republic

^m Universidad San Francisco de Quito, Quito, Ecuador

ⁿ Laboratoire de Physique Corpusculaire, IN2P3-CNRS, Université Blaise Pascal, Clermont-Ferrand, France

^o Laboratoire de Physique Subatomique et de Cosmologie, IN2P3-CNRS, Université de Grenoble I, Grenoble, France

^p CPPM, IN2P3-CNRS, Université de la Méditerranée, Marseille, France

^q IN2P3-CNRS, Laboratoire de l'Accélérateur Linéaire, Orsay, France

^r LPNHE, IN2P3-CNRS, Universités Paris VI and VII, Paris, France

^s DAPNIA/Service de Physique des Particules, CEA, Saclay, France

^t IReS, IN2P3-CNRS, Université Louis Pasteur, Strasbourg, France, and Université de Haute Alsace, Mulhouse, France

^u Institut de Physique Nucléaire de Lyon, IN2P3-CNRS, Université Claude Bernard, Villeurbanne, France

^v III. Physikalisches Institut A, RWTH Aachen, Aachen, Germany

^w Physikalisches Institut, Universität Bonn, Bonn, Germany

^x Physikalisches Institut, Universität Freiburg, Freiburg, Germany

^y Institut für Physik, Universität Mainz, Mainz, Germany

^z Ludwig-Maximilians-Universität München, München, Germany

^{aa} Fachbereich Physik, University of Wuppertal, Wuppertal, Germany

^{ab} Panjab University, Chandigarh, India

^{ac} Delhi University, Delhi, India

^{ad} Tata Institute of Fundamental Research, Mumbai, India

^{ae} University College Dublin, Dublin, Ireland

^{af} Korea Detector Laboratory, Korea University, Seoul, South Korea

^{ag} SungKyunKwan University, Suwon, South Korea

^{ah} CINVESTAV, Mexico City, Mexico

^{ai} FOM-Institute NIKHEF and University of Amsterdam/NIKHEF, Amsterdam, The Netherlands

^{aj} Radboud University Nijmegen/NIKHEF, Nijmegen, The Netherlands

^{ak} Joint Institute for Nuclear Research, Dubna, Russia

^{al} Institute for Theoretical and Experimental Physics, Moscow, Russia

^{am} Moscow State University, Moscow, Russia

^{an} Institute for High Energy Physics, Protvino, Russia

^{ao} Petersburg Nuclear Physics Institute, St. Petersburg, Russia

^{ap} Lund University, Lund, Sweden, Royal Institute of Technology and Stockholm University, Stockholm, Sweden

^{aq} Uppsala University, Uppsala, Sweden

^{ar} Physik Institut der Universität Zürich, Zürich, Switzerland

^{as} Lancaster University, Lancaster, United Kingdom

^{at} Imperial College, London, United Kingdom

^{au} University of Manchester, Manchester, United Kingdom

^{av} University of Arizona, Tucson, AZ 85721, USA

^{aw} Lawrence Berkeley National Laboratory and University of California, Berkeley, CA 94720, USA

^{ax} California State University, Fresno, CA 93740, USA

^{ay} University of California, Riverside, CA 92521, USA

^{az} Florida State University, Tallahassee, FL 32306, USA

^{ba} Fermi National Accelerator Laboratory, Batavia, IL 60510, USA

^{bb} University of Illinois at Chicago, Chicago, IL 60607, USA

- ^{bc} Northern Illinois University, DeKalb, IL 60115, USA
^{bd} Northwestern University, Evanston, IL 60208, USA
^{bc} Indiana University, Bloomington, IN 47405, USA
^{bf} University of Notre Dame, Notre Dame, IN 46556, USA
^{bg} Iowa State University, Ames, IA 50011, USA
^{bh} University of Kansas, Lawrence, KS 66045, USA
^{bi} Kansas State University, Manhattan, KS 66506, USA
^{bj} Louisiana Tech University, Ruston, LA 71272, USA
^{bk} University of Maryland, College Park, MA 20742, USA
^{bl} Boston University, Boston, MA 02215, USA
^{bm} Northeastern University, Boston, MA 02115, USA
^{bn} University of Michigan, Ann Arbor, MI 48109, USA
^{bo} Michigan State University, East Lansing, MI 48824, USA
^{bp} University of Mississippi, University, MS 38677, USA
^{bq} University of Nebraska, Lincoln, NB 68588, USA
^{br} Princeton University, Princeton, NJ 08544, USA
^{bs} State University of New York, Buffalo, NY 14260, USA
^{bt} Columbia University, New York, NY 10027, USA
^{bu} University of Rochester, Rochester, NY 14627, USA
^{bv} State University of New York, Stony Brook, NY 11794, USA
^{bw} Brookhaven National Laboratory, Upton, NY 11973, USA
^{bx} Langston University, Langston, OK 73050, USA
^{by} University of Oklahoma, Norman, OK 73019, USA
^{bz} Oklahoma State University, Stillwater, OK 74078, USA
^{ca} Brown University, Providence, RI 02912, USA
^{cb} University of Texas, Arlington, TX 76019, USA
^{cc} Southern Methodist University, Dallas, TX 75275, USA
^{cd} Rice University, Houston, TX 77005, USA
^{ce} University of Virginia, Charlottesville, VA 22901, USA
^{cf} University of Washington, Seattle, WA 98195, USA

Received 4 May 2006; received in revised form 5 July 2006; accepted 13 July 2006

Available online 24 July 2006

Editor: L. Rolandi

Abstract

We present the measurement of $R = \mathcal{B}(t \rightarrow Wb)/\mathcal{B}(t \rightarrow Wq)$ in $p\bar{p}$ collisions at $\sqrt{s} = 1.96$ TeV, using 230 pb^{-1} of data collected by the DØ experiment at the Fermilab Tevatron Collider. We fit simultaneously R and the number ($N_{t\bar{t}}$) of selected top quark pairs ($t\bar{t}$), to the number of identified b -quark jets in events with one electron or one muon, three or more jets, and high transverse energy imbalance. To improve sensitivity, kinematical properties of events with no identified b -quark jets are included in the fit. We measure $R = 1.03^{+0.19}_{-0.17}$ (stat + syst), in good agreement with the standard model. We set lower limits of $R > 0.61$ and $|V_{tb}| > 0.78$ at 95% confidence level.

© 2006 Elsevier B.V. All rights reserved.

PACS: 12.15.Hh; 14.65.Ha

Within the standard model (SM), the top quark decays 99.8% of the time to a W boson and a b quark, with the ratio $R = \mathcal{B}(t \rightarrow Wb)/\mathcal{B}(t \rightarrow Wq)$ (here q refers to d , s , or b quarks) expressible in terms of the Cabbibo–Kobayashi–Maskawa (CKM) matrix elements [1] $R = \frac{|V_{tb}|^2}{|V_{tb}|^2 + |V_{ts}|^2 + |V_{td}|^2}$. The unitarity of the CKM matrix and experimental constraints on its elements [2] yield the SM prediction $0.9980 < R < 0.9984$ at the 90% C.L. Nevertheless, a fourth generation of quarks or non-SM

processes in the production or decay of the top quark could lead to significant deviations from the SM. So far, measurements of R by the CDF Collaboration [3,4] have not established a deviation of R from unity.

In the present analysis, we assume that the top quark decays into a W boson, but that the associated quark can be d , s , or b . Lepton + jets final states arise in $t\bar{t}$ when one W boson decays leptonically and the other into a $q\bar{q}'$ pair. About 6% of the signal arises from $t\bar{t}$ events in which both W bosons decay leptonically, but one charged lepton is not reconstructed, while additional jets are produced by initial or final state radiation. In this Letter, we report the measurement of R in the lepton (electron or muon) + jets channel (ℓ + jets). The lepton can come either from a direct W decay or from $W \rightarrow \tau \rightarrow e/\mu$. We use b -jet identification (b -tagging) techniques, exploiting the long life-

* Corresponding author.

E-mail address: cclement@cern.ch (C. Clément).

¹ On leave from IEP SAS Kosice, Slovakia.

² Visitor from Purdue University Calumet, Hammond, IN, USA.

³ Visitor from Helsinki Institute of Physics, Helsinki, Finland.

time of B hadrons, to separate $t\bar{t}$ events from the background processes. The data were collected by the DØ experiment from August 2002 through March 2004, and correspond to an integrated luminosity of 230 pb^{-1} .

The DØ detector incorporates a tracking system, calorimeters, and a muon spectrometer [5]. The tracking system is made up of a silicon micro-strip tracker (SMT) and a central fiber tracker (CFT), located inside a 2 T superconducting solenoid. The tracking system provides efficient charged particle detection in the pseudorapidity region $|\eta| < 3$.⁴ The SMT strip pitch of 50–80 μm allows a precise determination of the primary interaction vertex (PV) and an accurate measurement of the impact parameter of a track relative to the PV.⁵ These are key components of the lifetime-based b -tagging algorithms. The PV is required to be within the fiducial region of the SMT and to contain at least three tracks. The calorimeter consists of a barrel section covering $|\eta| < 1.1$, and two end-caps extending the coverage to $|\eta| \approx 4.2$. The muon spectrometer surrounds the calorimeter and consists of three layers of drift chambers and several layers of scintillators [6]. A 1.8 T iron toroidal magnet is located outside the innermost layer of the muon system. The luminosity is calculated from the rate of $p\bar{p}$ inelastic collisions, detected by two arrays of scintillation counters mounted close to the beam-pipe on the front surfaces of the calorimeter end-caps.

We select data in the electron and muon decay channels by requiring an isolated electron with $p_T > 20 \text{ GeV}$ and $|\eta| < 1.1$, or an isolated muon with $p_T > 20 \text{ GeV}$ and $|\eta| < 2.0$. The lepton isolation criteria are based on calorimeter and tracking information. More details on lepton identification and trigger requirements are available in Ref. [7]. In both channels, we require the missing transverse energy (\cancel{E}_T) to exceed 20 GeV and not be collinear with the direction of the lepton projected on the transverse plane. The candidate events must be accompanied by jets with $p_T > 15 \text{ GeV}$ and rapidity $|y| < 2.5$ (footnote 4). Jets are defined using a cone algorithm with radius $\Delta\mathcal{R} = 0.5$ [8].

We use a secondary vertex tagging (SVT) algorithm to reconstruct displaced vertices produced by the decay of B hadrons inside jets. Secondary vertices are reconstructed from two or more tracks satisfying: $p_T > 1 \text{ GeV}$, ≥ 1 hits in the SMT detector, and impact parameter significance $d_{ca}/\delta_{dca} > 3.5$ (footnote 5). Tracks identified as arising from K_S^0 or Λ decays or from γ conversions are not used. If the secondary vertex reconstructed within a jet has a decay-length significance $L_{xy}/\delta_{Lxy} > 7$,⁶ the jet is defined as b -tagged. Events with exactly 1 (≥ 2) b -tagged jets are referred to as 1-tag (2-tag)

⁴ Rapidity y and pseudorapidity η are defined as functions of the parameter β and polar angle θ w.r.t. the proton beam line, as $y(\theta, \beta) \equiv \frac{1}{2} \ln[(1 + \beta \cos \theta)/(1 - \beta \cos \theta)]$ and $\eta(\theta) \equiv y(\theta, 1)$, where β is the ratio of a particle's momentum to its energy.

⁵ Impact parameter is defined as the distance of closest approach (d_{ca}) of the track to the primary vertex in the plane transverse to the beam line. Impact parameter significance is defined as d_{ca}/δ_{dca} , where δ_{dca} is the error on d_{ca} .

⁶ Decay length L_{xy} is defined as the distance from the primary to the secondary vertex in the plane transverse to the beam line. Decay length significance is defined as L_{xy}/δ_{Lxy} , where δ_{Lxy} is the uncertainty on L_{xy} .

events. Events with no b -tagged jets are referred to as 0-tag events. A prediction for the number of background events and the fractions of $t\bar{t}$ events in the 0, 1, and 2-tag samples require the probabilities for different types of jets (b -, c -, and light-quark jets) to be b -tagged. The calculation of these probabilities is presented in Ref. [13]. We fit simultaneously R and the total number of $t\bar{t}$ events in the 0, 1, and 2-tag samples ($N_{t\bar{t}}$) to the number of observed 1-tag and 2-tag events, and, in 0-tag events, to the shape of a discriminant variable \mathcal{D} that exploits kinematic differences between the backgrounds and the $t\bar{t}$ signal.

The main background in this analysis is from the production of leptonically decaying W bosons produced in association with jets ($W + \text{jets}$). Most of the jets accompanying the W boson originate from u , d , and s quarks and gluons ($W + \text{light jets}$). Between 2% and 14% of $W + \text{jets}$ events contain heavy-flavor jets, arising from gluon splitting into $b\bar{b}$ or $c\bar{c}$ ($Wb\bar{b}$ or $Wc\bar{c}$, respectively). About 5% of the $W + \text{jets}$ events contain a single c quark that originates from W -boson radiation from an s quark in the proton or anti-proton sea ($s \rightarrow Wc$). A sizable background arises from strong production of two or more jets (“multijets”), with one of the jets misidentified as an isolated lepton, and accompanied by large \cancel{E}_T resulting from mismeasurement of jet energies. Significantly smaller contributions to the selected sample arise from $Z + \text{jets}$, WW , WZ , ZZ , and single top quark production. Together, these five smaller backgrounds are expected to contribute from 1% to 7% of the selected sample, depending on the number of b -tagged jets, and are referred to below as “other” backgrounds.

Normalization of the backgrounds begins with the determination of the number of multijet events in the selected sample. The multijet background is determined using control data samples and probabilities for jets to mimic isolated lepton signatures, also derived from data [7]. Subtracting this background also provides the fraction of events with a truly isolated high- p_T lepton (i.e., $t\bar{t}$ and all backgrounds, except multijets). The contributions from single top quark, $Z + \text{jets}$, and diboson production are determined from Monte Carlo simulation (MC). The remainder corresponds either to $t\bar{t}$ or $W + \text{jet}$ production. The $W + \text{jets}$ background normalization is constrained by the untagged data, as a function of jet multiplicity, while its flavor composition is taken from MC. The signal and background processes are generated using ALPGEN [9] with $m_t = 175 \text{ GeV}$. PYTHIA [10] is used for fragmentation and decay. B hadron decays are modeled via EVTGEN [11]. A full detector simulation is performed using GEANT [12].

In an analysis based on the SM, with $R \approx 1$, the $t\bar{t}$ event tagging probabilities are computed assuming that each of the signal events contains two b -jets [13]. In the present analysis, the top quark can also decay into a light quark (d or s) and a W boson. The ratio R determines the fraction of $t\bar{t}$ events with 0, 1, and 2 b -jets and therefore how $t\bar{t}$ events are distributed among the 0, 1, and 2-tag samples. In order to derive the $t\bar{t}$ event tagging probability as a function of R , we determine the tagging probability for the three following scenarios (i) $t\bar{t} \rightarrow W^+bW^-b$ (to be referred to as $tt \rightarrow bb$), (ii) $t\bar{t} \rightarrow W^+bW^-q_l$ or its charge conjugate (referred to as $tt \rightarrow bq_l$), and (iii) $t\bar{t} \rightarrow W^+q_lW^-q_l$ (referred to as $tt \rightarrow q_lq_l$), where q_l denotes either a d or s

Table 1
Observed number of events, predicted backgrounds and fitted $N_{t\bar{t}}$

$\ell + 3$ jets	0-tag	1-tag	≥ 2 -tag
$W +$ jets	1032 ± 38	34 ± 5	2.4 ± 0.4
Multi-jet	192 ± 23	8.3 ± 1.5	$0.1^{+0.3}_{-0.1}$
Other bkg	18.4 ± 1.3	4.3 ± 0.3	0.7 ± 0.1
Fitted $t\bar{t}$	32.4 ± 1.6	32.3 ± 1.6	8.2 ± 0.5
Total	1275 ± 44	79 ± 5	11.4 ± 0.8
Observed	1277	79	9
$\ell + \geq 4$ jets	0-tag	1-tag	≥ 2 -tag
$W +$ jets	193 ± 17	8.8 ± 1.2	0.7 ± 0.1
Multi-jet	65 ± 9	4.1 ± 1.1	0.0 ± 0.4
Other bkg	2.9 ± 0.4	1.2 ± 0.2	0.2 ± 0.1
Fitted $t\bar{t}$	35.6 ± 2.8	41.5 ± 3.3	13.5 ± 1.4
Total	297 ± 19	56 ± 4	14.4 ± 1.4
Observed	291	62	14

quark. The probabilities $P_{n_{\text{tag}}}$ to observe $n_{\text{tag}} = 0, 1$, or ≥ 2 b -tagged jets are computed separately for the three types of $t\bar{t}$ events, using the probabilities for each type of jet (b , c , or light-quark jet) to be b -tagged. The probabilities $P_{n_{\text{tag}}}$ in the three scenarios are then combined to obtain the $t\bar{t}$ tagging probability as a function of R , $P_{n_{\text{tag}}}(tt) = R^2 P_{n_{\text{tag}}}(tt \rightarrow bb) + 2R(1-R)P_{n_{\text{tag}}}(tt \rightarrow bq\ell) + (1-R)^2 P_{n_{\text{tag}}}(tt \rightarrow q\ell q\ell)$, where the subscript n_{tag} runs over 0, 1, and ≥ 2 tags. Table 1 compares the observed number of events in the 0, 1, and 2-tag samples with the sum of the predicted backgrounds and the fitted number of $t\bar{t}$ events.

The fraction of $t\bar{t}$ events in the $\ell + \geq 4$ jets ($\ell + 3$ jets) 0-tag sample changes from 10% (2%) for $R = 1$ to 22% (4%) for $R = 0$. The size of this contribution is of the order of the Poisson uncertainty on the number of events in the 0-tag sample. Therefore the number of observed 0-tag events is a poor constraint on R and $N_{t\bar{t}}$. We achieve a tighter constraint on the number of $t\bar{t}$ events in the 0-tag sample by constructing a discriminant function \mathcal{D} for 0-tag events in the $\ell + \geq 4$ jets sample, that combines kinematical event properties to discriminate between $t\bar{t}$ signal and $W +$ jets background. The signal to background ratio in the $\ell + 3$ jets, 0-tag sample is five times smaller than in the corresponding ≥ 4 jets sample. Therefore we do not consider such a discriminant for $\ell + 3$ jets, 0-tag events. We select four variables that provide good discrimination between signal and background and that are well modeled by the MC. The discriminant function is built from: (i) the event sphericity \mathcal{S} , constructed from the four-momenta of the jets, (ii) the event centrality \mathcal{C} , defined as the ratio of the scalar sum of the p_T of the jets to the scalar sum of the energies of the jets, (iii) $K'_{T\text{min}} = \Delta\mathcal{R}'_{jj\text{min}} p_T^{\text{min}} / E_T^W$, where $\Delta\mathcal{R}'_{jj\text{min}}$ is the minimum separation in $\eta - \phi$ space between pairs of jets, p_T^{min} is the p_T of the lower- p_T jet of that pair, and E_T^W is the scalar sum of the lepton transverse momentum and \cancel{E}_T , and (iv) $H'_{T2} = H_{T2} / H_z$, where H_{T2} is the scalar sum of the E_T for all jets excluding the leading jet and H_z is the scalar sum of the absolute value of the momenta of all the jets, the lepton and the neutrino along the

z -direction.⁷ Sphericity and centrality characterize the event shape and are described in Ref. [14]. In order to reduce the dependence on modeling of soft radiation and the underlying event, only the four highest- p_T jets are used to determine these variables.

The discriminant function is constructed using the method described in Ref. [15]. Neglecting correlations among the input variables x_1, x_2, \dots , the discriminant function can be approximated by the expression

$$\mathcal{D} = \frac{\prod_i s_i(x_i)/b_i(x_i)}{\prod_i s_i(x_i)/b_i(x_i) + 1}, \quad (1)$$

where $s_i(x_i)$ and $b_i(x_i)$ are the normalized distributions of variable x_i for signal and background, respectively. As constructed, the discriminant peaks near zero for background, and near one for signal. The shapes of the discriminant for $t\bar{t}$ and $W +$ jets events are derived from MC.

The shape of the discriminant for the multijet background is obtained from a control data sample, selected by requiring that the lepton candidates fail the isolation criteria. The other backgrounds ($Z +$ jets, diboson, and single top quark) have discriminant distributions close to those of the $W +$ jet events, and contribute to 1% of the 0-tag sample. In the final fit, we assume that these processes have the same discriminants as the $W +$ jets events. The background normalization in the $\ell + \geq 4$ jets, 0-tag sample is extracted from the discriminant fit rather than from MC. We verify that the kinematic variables used in the discriminant are well modeled by the simulation by comparing data and MC distributions in two control samples with little $t\bar{t}$ content: $\ell + 2$ jets and $\ell + 3$ jets before tagging. In $\ell + 2$ jets events, the fraction of $t\bar{t}$ events is negligible, whereas it makes up about 5% of the $\ell + 3$ jets events.

In order to measure R and $N_{t\bar{t}}$, we perform a binned maximum likelihood fit. The data are binned in thirty bins: (i) twenty bins of the discriminant \mathcal{D} in the $e + \geq 4$ jets and $\mu + \geq 4$ jets, 0-tag samples, (ii) two bins for the two 0-tag samples in $e + 3$ jets and $\mu + 3$ jets, (iii) four bins for the four 1-tag samples (electron or muon and 3 or 4 jets), and (iv) four bins for the four 2-tag samples (electron or muon and 3 or 4 jets). In each bin, we predict the number of events that corresponds to the sum of the expected background and signal. The signal contribution is a function of R and $N_{t\bar{t}}$. To predict the number of events in each bin of the discriminant \mathcal{D} , we use its expected distribution for $W +$ jets background and $t\bar{t}$ signal. As described earlier, the normalization of the multijet background is estimated by counting events in orthogonal control samples. Statistical fluctuations in the number of events in the control samples are taken into account. We incorporate systematic uncertainties into the likelihood by using nuisance parameters [16]. All pre-selection efficiencies, tagging probabilities, and shapes of the discriminant \mathcal{D} are functions of the nuisance parameters. The likelihood contains one Gaussian term for each nuisance parameter. The value of R that maximizes the total likelihood is

⁷ The neutrino momentum along the z direction (p_z^{ν}) is determined by assuming that each event contains one W boson. The W mass is used as an additional constraint to derive p_z^{ν} . The solution with the smallest $|p_z^{\nu}|$ is chosen.

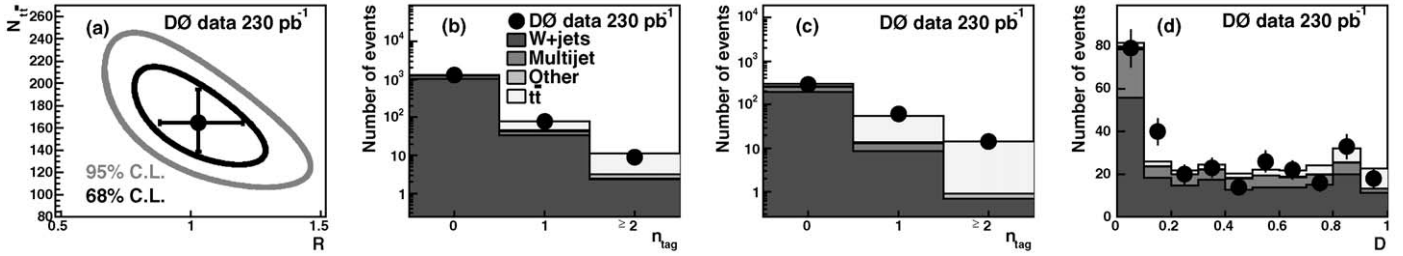


Fig. 1. (a) The 68% and 95% statistical confidence contours in the $(R, N_{t\bar{t}})$ plane. The point indicates the best fit to data. Observed number of events and fitted sample composition in the 0, 1, and 2-tag samples (b) in the $\ell + 3$ jets sample and (c) in the $\ell + \geq 4$ jets sample. (d) Observed and fitted distribution of the discriminant \mathcal{D} .

Table 2
Summary of statistical and systematic uncertainties on R

Uncertainties on R		
Statistical	+0.17	-0.15
b -tagging efficiency	+0.06	-0.05
Background modeling	+0.05	-0.04
Jet identification and energy calibration	+0.04	-0.03
Multijet background	±0.02	
Total error	+0.19	-0.17

$R = 1.03^{+0.19}_{-0.17}$ (stat + syst), in good agreement with the SM expectation. A summary of statistical and systematic uncertainties is given in Table 2. The fit also yields the total number of $t\bar{t}$ events in the 0, 1, and 2-tag samples, $N_{t\bar{t}} = 163^{+29}_{-27}$ (stat). The result of the two-dimensional fit is shown in the $(R, N_{t\bar{t}})$ plane in Fig. 1(a), with the 68% and 95% contours of statistical confidence. In Fig. 1(b) and (c), we compare the observed number of events to the sum of the predicted backgrounds and the fitted $t\bar{t}$ contribution, in the 0, 1 and 2-tag samples for events with 3 jets and ≥ 4 jets. In Fig. 1(d), we compare the observed distribution of the discriminant \mathcal{D} with the corresponding distribution for the sum of the predicted backgrounds and the fitted $t\bar{t}$ contribution.

We extract lower limits on R and the CKM matrix element $|V_{tb}|$ assuming $|V_{tb}| = \sqrt{R}$. Using a Bayesian approach with the prior $\pi(R) = 1$ for $0 \leq R \leq 1$ and $\pi(R) = 0$ otherwise, we obtain $R > 0.78$ at the 68% C.L. and $R > 0.61$ at the 95% C.L. For the CKM matrix element $|V_{tb}|$, we obtain $|V_{tb}| > 0.88$ at 68% C.L., and $|V_{tb}| > 0.78$ at the 95% C.L.

In summary, we performed the most accurate measurement of R to date, $R = 1.03^{+0.19}_{-0.17}$ (stat + syst), in good agreement with the SM.

Acknowledgements

We thank the staffs at Fermilab and collaborating institutions, and acknowledge support from the DOE and NSF

(USA); CEA and CNRS/IN2P3 (France); FASI, Rosatom and RFBR (Russia); CAPES, CNPq, FAPERJ, FAPESP and FUNDUNESP (Brazil); DAE and DST (India); Colciencias (Colombia); CONACyT (Mexico); KRF and KOSEF (Korea); CONICET and UBACyT (Argentina); FOM (The Netherlands); PPARC (United Kingdom); MSMT (Czech Republic); CRC Program, CFI, NSERC and WestGrid Project (Canada); BMBF and DFG (Germany); SFI (Ireland); The Swedish Research Council (Sweden); Research Corporation; Alexander von Humboldt Foundation; and the Marie Curie Program.

References

- [1] N. Cabibbo, Phys. Rev. Lett. 10 (1963) 531; M. Kobayashi, T. Maskawa, Prog. Theor. Phys. 49 (1973) 652.
- [2] S. Eidelman, et al., Phys. Lett. B 592 (2004) 1.
- [3] CDF Collaboration, T. Affolder, et al., Phys. Rev. Lett. 86 (2001) 3233.
- [4] CDF Collaboration, T. Affolder, et al., Phys. Rev. Lett. 95 (2005) 102002.
- [5] DØ Collaboration, V. Abazov, et al., physics/0507191, Nucl. Instrum. Methods Phys. Res. A (2006), in press.
- [6] V. Abazov, et al., Nucl. Instrum. Methods Phys. Res. A 552 (2001) 372–398.
- [7] DØ Collaboration, V. Abazov, et al., Phys. Lett. B 626 (2005) 45.
- [8] We use the iterative, seed-based cone algorithm including midpoints, as described in G.C. Blazey, et al., in: U. Baur, R.K. Ellis, D. Zeppenfeld, (Eds.), Proceedings of the Workshop: QCD and Weak Boson Physics in Run II, FERMILAB-PUB-00-297, 2000, p. 47.
- [9] M.L. Mangano, et al., JHEP 0307 (2003) 001.
- [10] T. Sjöstrand, et al., Comput. Phys. Commun. 135 (2001) 238.
- [11] D.J. Lange, Nucl. Instrum. Methods Phys. Res. A 462 (2001) 152.
- [12] R. Brun, F. Carminati, CERN Program Library Long Writeup W5013, 1993, unpublished.
- [13] DØ Collaboration, V. Abazov, et al., Phys. Lett. B 626 (2005) 35.
- [14] V. Barger, J. Ohnemus, R.J.N. Phillips, Phys. Rev. D 48 (1993) R3953.
- [15] DØ Collaboration, B. Abbott, et al., Phys. Rev. D 58 (1998) 052001.
- [16] E.T. Jaynes, Probability Theory, Cambridge Univ. Press, Cambridge, 2003.